M.F.A. SABANA, N. MUHAYAT, TRIYONO

ISSN 0543-5846
METABK 62(3-4) 371-374 (2023)
UDC – UDK 669.14.018:621.791.052.004.67:620.18:620.178.1=111

EFFECT OF THE REPAIR WELDING PROCESS ON THE MICROSTRUCTURE AND HARDNESS OF THE T-JOINT S355J2+N STEEL

Received – Primljeno: 2023-01-26
Accepted – Prihvaćeno: 2023-04-20
Original Scientific Paper – Izvorni znanstveni rad

The purpose of this research is to determine effect of the repair welding process on the microstructure and hardness of the T-joint S355J2+N steel. This process was carried out by moving the welding position 10 mm from the initial position using Gas Metal Arc Welding (GMAW) with AWS ER-706S filler metal at a diameter of 1.2 mm. The result showed that the repair welding process causes changes in the microstructure due to repeated heating, thereby increasing the grain size of the microstructure with a decrease in hardness.

Keywords: steel S355J2+N, GMAW, repair welding, microstructure, hardness

INTRODUCTION

S355J2+N is a high-strength steel with low carbon content often used as a vehicle frame due to its dynamic loads and ability to work at low temperatures. Its strength is obtained from heat treatment in the manufacturing process [1]. Furthermore, the most frequent type of welding used in the vehicle manufacturing industry is Gas Metal Arc Welding (GMAW) because it is efficient with the electrode wire fed and melted by the arc semi-automatically. [2]. GMAW can also be applied to ferrous and non-ferrous materials [3]. However, it is more expensive and complex due to the use of shielding gas [4].

Errors, such as misplaced joints and types, as well as sizes and defects of joints in the welding process, prevents it from meeting the specified criteria [5]. The repair welding process can improve production time and cost efficiency by eliminating the need to replace part that does not comply with the specified criteria [6]. In general, repair welding results in a decrease in hardness. This is because the workpiece is subjected to repeated heat from the initial and repair welding processes, as well as the specimen's microstructure, especially in the heat-affected area, which becomes rough. [6-8]. However, data on the effect of the repair welding process on the material properties of S355J2+N structural steel is still limited. The scarcity is because the mechanism for strengthening the steel is heat treatment, which can damage its strength.

EXPERIMENTAL PROCEDURES

This research was carried out using the S355J2+N steel plate with dimensions 400 x 150 x 25 mm. The electrodes used in the welding process are AWS ER 70S-6, with a diameter of 1,2 mm. Table 1 describes the chemical content of S355J2+N steel and AWS ER 70S-6 filler.

The welding process is carried out with a joint design, as shown in Figure 1. Furthermore, it uses a GMAW OTC type XD350S machine with the parameters shown in Table 2. After the welding is completed, the joint is repaired by a series of cutting, grinding, and rewelding processes with the joint position shifted 10 mm, as shown in Figure 2. The rewelding process comprises similar parameters to the initial phase. Furthermore, the repair welding process is characterized by observing the macro and the microstructures as well as the hardness test around the joints. The same characterization was also performed on the initial welded joints as a comparison. Hardness tests were conducted at a depth of 5 mm, 6 mm, 7 mm, and 8 mm, as shown in Figure 3.

Table 1 **Chemical composition of materials /wt. %**

Element	Materials	
	S355J2+N	ER70S-6
P	0,005	0,025
C	0,15	0,15
S	0,001	0,035
Mn	1,42	1,85
Cu	0,01	0,85
Si	0,4	1,15
Cr	0,02	<0,5
Mo	0,002	<0,5
Nb	0,029	-
Ni	0,16	<0,5
Ti	0,003	-
V	0,058	-
Fe	Balance	Balance

Triyono (e-mail: triyono74@staff.uns.ac.id), M.F.A. Sabana, N. Muhayat, Mechanical Engineering Department, Universitas Sebelas Maret, Surakarta, Indonesia

Table 2 **Welding parameters**

Welding Process	Semi-automatic (GMAW)
Type of Joint	Tee Joint (Multipass)
Basic Material	S355J2+N
Filler Metal	Type : AWS ER70S-6
	Diameter : 1,2 mm
Shielding Gas	Type : Ar (82 %) + CO_2 (18 %)
	Flow : 15-17 L/min
Current	Polarity : DC +
	Ampere : 225–275 A
Voltage	22-27 V

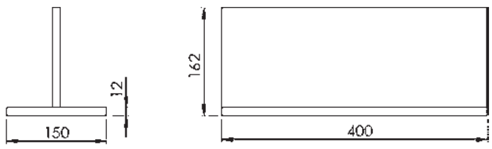

Figure 1 Weld joint configuration.

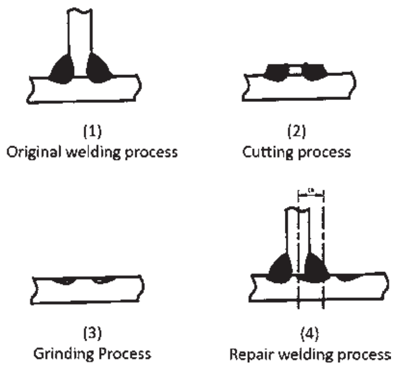

Figure 2 Repair welding process

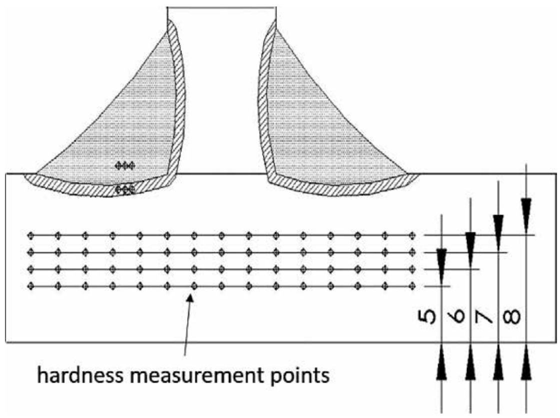

Figure 3 Position of hardness testing point (mm)

RESULTS AND DISCUSSION

Observation of the parent metal microstructure indicated the presence of ferrite (F) and pearlite (P) phases. Borko et al, (2018) stated that the ferrite content in S355J2+N steel can reach 90 % [9]. The morphology of this phase belongs to the ferrite columnar phase with small grain sizes and elongated grooves due to the hot rolling treatment during the production process [10].

Figures 4 and 5 show a comparison of the original and repaired T-welded joints macrostructure. The original consisted of a fillet area on either side of the web where the weld metal penetrated both the web and the flange. The Heat-Affected Zone (HAZ) occurs around the weld metal, while the macrostructure has the same area as before the repair. However, due to the repair, there are areas of former weld metal and HAZ of the original joint on the flange, which is also re-heated during the repair welding process.

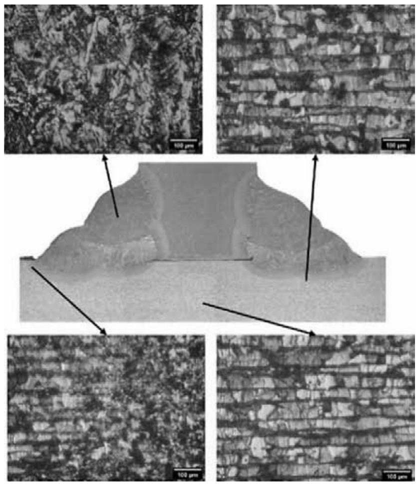

Figure 4 Macro and microstructure of original welded joints

Figures 4 and 5 also show a comparison of the microstructure in the important areas, as indicated by the arrows. The HAZ on the original welding specimen consists of ferrite and pearlite phases. Furthermore, the originally elongated microstructure turned into finer grains with random configurations. The microstructure in this area is dominated by the ferrite phase, while those in the weld metal of the original welding specimen comprise small percentages of ferrite and pearlite. The ferrite phase in this area is of the Widmanstatten Ferrite (WF) and Acicular Ferrite (AF)[11,12].

The repair welding process causes the area to be subjected to repeated thermal cycles, increasing amount and size of grains near the weld zone [7, 13]. The microstructure in the HAZ repair welding area consists of ferrite and pearlite with fine grains. It is the first welding area consisting of ferrite, pearlite, CF and AF phases. Additionally, the microstructure of the weld metal in repair welding is dominated by small percentages of ferrite and pearlite phases. The ferrite phase in this area is of the Grain Boundary Ferrite (GF) and acicular ferrite (AF) types [11, 12, 14].

The results of the original weld joint hardness test without repair are shown in Figure 6. The original welding metal area has the lowest amount of hardness. Its average at depths of 8 and 7 mm, were 148,83 HV and 157,94 HV, respectively. Furthermore, the microstructure at 8 mm and 7 mm depths is coarse and small. Its average at a depth of 5 and 6 mm was 157,50 HV and 157,88 HV, respectively, which was almost the same as the hardness at 7 mm. This is because the microstructure size in this area is the same as at a depth of 7 mm.

Figure 7 shows the results of the repaired welded joint area hardness test. The lowest average hardness is

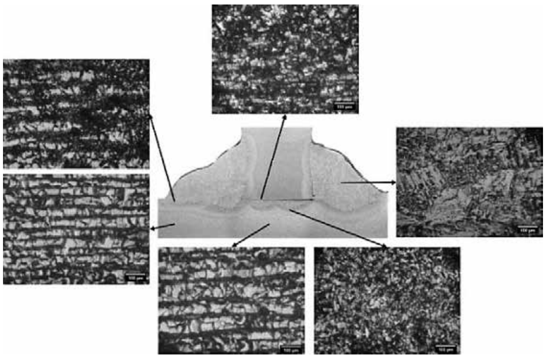

Figure 5 Macro and microstructure repair welding

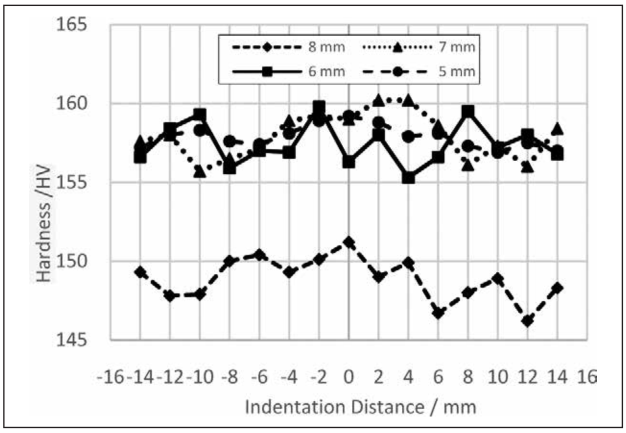

Figure 6 Original welding hardness

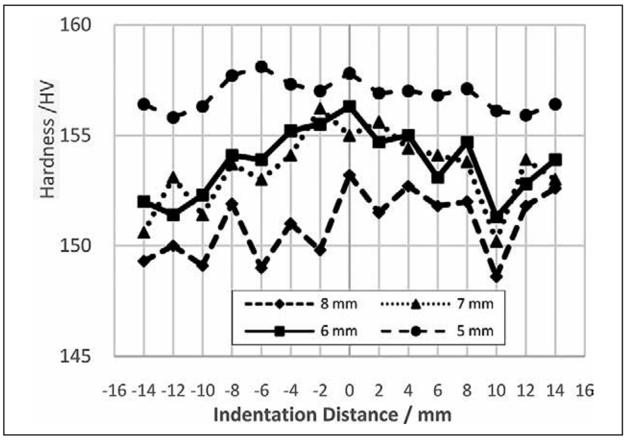

Figure 7 Repair welding hardness

at a depth of 8 mm, with a value of 151,05 HV. This is because, in this area, the microstructure is large due to the heat input received during the repair welding processes. Therefore, due to the repeated heat input during repair welding, the average hardness in the depth area of less than 8 mm is lower compared to the initial weld joint without repair. The lowest hardness in each depth area is located at a distance of +10 mm from the center of the joint. This is because that area gets twice the heat input of the original and repair welding processes.

The average hardness of the original welding specimen's HAZ was 155,9 HV. This is lower than the hardness of the repair welding specimen at 156,73 HV. The HAZ microstructure on the original welding specimen is finer than the HAZ repair welding microstructure.

The highest hardness is in the weld metal (WM) area because the filler used is ER70S-6, which has higher mechanical properties than S355J2+N steel. The average hardness in the WM original weld and repair welding area is 219,1 HV and 215,26 HV, respectively, as shown in Figure 8. The increase in hardness is caused by the type of phase contained in the area. WM original welding comprises AF and WF phases, while WM repair welding consists of AF and grain boundary ferrite. Therefore, the hardness of WM original welding is due to the higher content of Acicular Ferrite (AF) and Widmanstatten Ferrite (WF)[15].

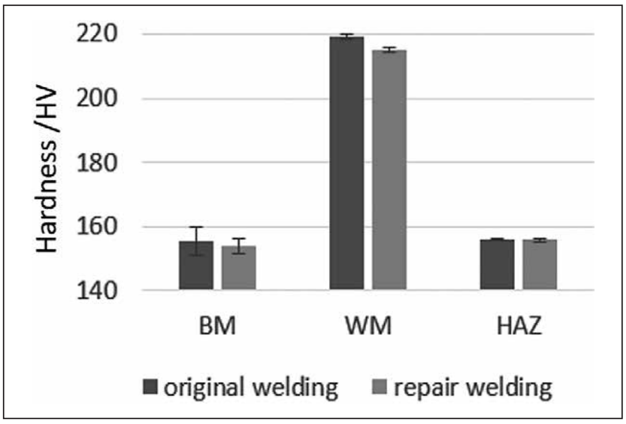

Figure 8 Average hardness in the area of base metal, HAZ, and weld metal

CONCLUSIONS

The microstructure of original welding HAZ is dominated by the ferrite phase, while those of original weld metal comprise small percentages of ferrite and pearlite. The repair welding process causes the microstructure to expand and become coarse due to repeated heat input. It causes the repair welding hardness to be lower than the original welding hardness in both HAZ and WM. Furthermore, the flange area up to 7 mm in depth has an almost uniform hardness, which becomes random after the repair welding process.

Acknowledgments

The authors are grateful to Universitas Sebelas Maret Surakarta for financing this research through HRG Research Grant 2023.

REFERENCES

[1] V. Milovanovi, M. Živkovi, G. Jovi, A. Dišic, Experimental determination of fatigue properties and fatigue life of S355J2 + N steel grade, , Materials Today, 12 (2019) 455–461 https://doi.org/10.1016/j.matpr.2019.03.149.

[2] Y. Cheng, R. Yu, Q. Zhou, H. Chen, W. Yuan, Y. Zhang, Real-time sensing of gas metal arc welding process – A literature review and analysis, Journal of Manufacturing Process, 70 (2021) 452–469 https://doi.org/10.1016/j.jmapro.2021.08.058.

[3] R. Thompson Martinez, G. Alvarez Bestard, S.C. Absi Alfaro, Two gas metal arc welding process dataset of arc parameters and input parameters, Data in Brief, 35 (2021), 106790, 1-7 https://doi.org/10.1016/j.dib.2021.106790.

[4] B. Mvola, P. Kah, Effects of shielding gas control: welded joint properties in GMAW process optimization, The International Journal of Advanced Manufacturing Technology, 88 (2017), 2369–2387 https://doi.org/10.1007/s00170-016-8936-2.

[5] M. Charkhi, D. Akbari, Experimental and numerical investigation of the effects of the pre-heating in the modification of residual stresses in the repair welding process, International Journal of Pressure Vessels and Piping, 171 (2019), 79–91 https://doi.org/10.1016/j.ijpvp.2019.02.006.

[6] J. Pikuła, M. Somozik, T. Pfeifer, The influence of manual metal arc multiple repair welding of long operated waterwall on the structure and hardness of the heat affected zone of welded joints, Archives of Metallurgy and Materials, 62 (2017), 327–333 https://doi.org/10.1515/amm-2017-0049.

[7] O.E. Vega, J.M. Hallen, A. Villagomez, A. Contreras, Effect of multiple repairs in girth welds of pipelines on the mechanical properties, Materials Characterization, 59 (2008), 1498–1507 https://doi.org/10.1016/j.matchar.2008.01.011.

[8] I. AghaAli, M. Farzam, M.A. Golozar, I. Danaee, The effect of repeated repair welding on mechanical and corrosion properties of stainless steel 316L, Materials and Design, 54 (2014), 331–341 https://doi.org/10.1016/j.matdes.2013.08.052.

[9] K. Borko, F. Pastorek, M.N. Jacková, B. Hadzima, Electrochemical properties of welded S355J2 steel before and after surface treatment by manganese phosphating, 34th Danubia Adria Symposium on Advances in Experimental Mechanics, Romania, 2018, 5, Materials Today, pp.26482–26488 www.materialstoday.com/proceedings www.sciencedirect.comwww.materialstoday.com/proceedings.

[10] T.˥ęzak, L.˺niezek, A Comparative LCF Study of S960QL High Strength Steel and S355J2 Mild Steel, 1st International Conference on Structural Integrity, Portugal, 2015, 114, Procedia Engineering, pp. 78–85 https://doi.org/10.1016/j.proeng.2015.08.044.

[11] D. Phelan, N. Stanford, R. Dippenaar, In situ observations of Widmanstätten ferrite formation in a low-carbon steel, Materials Science and Engineering A, 407 (2005), 127–134 https://doi.org/10.1016/j.msea.2005.07.015.

[12] B. Wang, Y. Zhang, F. Qiu, G. Cai, W. Cui, Z. Hu, H. Zhang, N. Tyrer, G.C. Barber, Role of trace nanoparticles in manipulating the widmanstatten structure of low carbon steel, Materials Letters, 306 (2022), 130853, 1-4 https://doi.org/10.1016/j.matlet.2021.130853.

[13] A. Yürük, B. Çevik, N. Kahraman, Analysis of mechanical and microstructural properties of gas metal arc welded dissimilar aluminum alloys (AA5754/AA6013), Materials Chemistry and Physics, 273 (2021), 1-13 https://doi.org/10.1016/j.matchemphys.2021.125117.

[14] M. Fattahi, N. Nabhani, M. Hosseini, N. Arabian, E. Rahimi, Effect of Ti-containing inclusions on the nucleation of acicular ferrite and mechanical properties of multipass weld metals, Micron, 45 (2013), 107–114. https://doi.org/10.1016/j.micron.2012.11.004.

[15] F. Liu, Q. Wang, J. Li, Y. Liu, T. He, G. Yuan, Systematic study on orientation relationships between acicular ferrite and Ti-Mg oxide at different cooling rates in low-carbon steel, Materials Characterization, 181 (2021), 111503, 1-16 https://doi.org/10.1016/j.matchar.2021.111503.

Note: The responsible English translator is the Native Proofreading Service - in Indonesia.